Direct Valorization of Recycled Palladium as Heterogeneous Catalysts for Total Oxidation of Methane

Michaël Martin Romo y Morales, Anthony Brunet-Manquat, Hadi Dib, Jean-luc Rousset, Franck Morfin, Laurence Burel, Damien Bourgeois, Helena Kaper

ChemCatChem
Research Article
doi.org/10.1002/cctc.202300354
Chemistry Europe
European Chemical Societies Publishing
www.chemcatchem.org

Special Collection

Direct Valorization of Recycled Palladium as Heterogeneous Catalysts for Total Oxidation of Methane

Michaël Martin Romo y Morales,[a, b] Anthony Brunet-Manquat,[a] Hadi Dib,[b] Jean-Luc Rousset,[c] Franck Morfin,[c] Laurence Burel,[c] Damien Bourgeois,*[a] and Helena Kaper*[b]

Electronic waste as an alternative source of palladium is used for the preparation of heterogeneous catalysts for methane oxidation. The strategy developed in this paper involves two steps: optimization of the leaching protocol to recover the Pd from the waste, and development of a suitable impregnation protocol directly from the leachate, which is a strongly acidic solution. The precipitation-deposition technique is particularly suitable for the preparation of catalysts from acidic media. The impact of Ba, Bi, and Ag impurities on the catalytic performance is studied on model catalysts. The presence of these elements and their impact on the catalytic properties are analyzed and discussed using X-ray diffraction, nitrogen physisorption, scanning and transmission electron microscopy. Through variation of the pH, the impurities co-deposited with Pd can be limited and the catalytic performance of catalysts derived from real waste can be greatly enhanced.

Introduction

Catalysis is at the heart of most industrial processes, and extensive R&D efforts are directed towards the development of better performing catalysts. Precious metals such as platinum group metals (PGM) take the lion's share of catalysed reactions because of their unique reactivity. However, their high prices make their applications often limited.[1] One solution is the development of new catalysts based on cheaper transition metals,[2] but complete substitution remains a long-term challenge. Catalysts embedding PGM can be regenerated and recycled, and metals of interest recovered, re-purified, and used directly to produce new catalysts. But all these metals are still coming initially from a natural ore deposit, and whatever the turnover of the recycling processes, stocks in metals decline – about 50% of the precious metals contained in converters end-up in exhaust dust – and have to be supplemented, without mentioning new needs.[3] A solution generally put forward in order to overcome the anticipated lack in natural resources is the exploitation of the so-called 'urban mine', i.e. our waste.[4] This solution is especially attractive in developed countries, since these 'consumers' societies generate lots of waste, and are poorly endowed with natural resources.[5] For instance, waste of electric and electronic equipment (e-waste) have been described to contain in average a 100 fold higher concentration in precious metals (gold, palladium…) than natural sources.[6] Nevertheless, today, recycling of e-waste remains low, and only gold-rich fractions are valued, through the complete successive separation of all present metals, which necessitate intensive purification sequences.[7] We recently demonstrated that it is possible to perform palladium-catalyzed reactions employing a pre-catalyst prepared from palladium(II) solutions mimicking those obtained during the processing of e-waste, bypassing all final isolation and purification steps.[8] Such an approach shortens the e-waste processing scheme, and minimizes associated secondary wastes. To our knowledge, although related approaches have recently emerged,[9] this is the only precedent on the preparation of active palladium catalysts from waste. A similar approach has been published in order to value copper also contained in e-waste,[10] but palladium still remains one of the most valuable metals neglected during e-waste reprocessing. Many catalytic processes using palladium rely on heterogeneous catalysts, and homogeneous Pd-catalysis thrives towards immobilization of Pd to improve recovery and re-use of Pd. We have started to adress the preparation of palladium-based supported catalysts directly from e-waste, with total oxidation of methane as one possible application. With the increase in natural gas as fuel in vehicles and stationary engines, the complete oxidation of methane as post-comubstion treatment is a very important aspect, as methane has a global warming potential 25 times higher than CO_2.[11] In general palladium or

[a] M. M. R. y Morales, A. Brunet-Manquat, D. Bourgeois
Laboratoire des Systèmes Hybrides pour la Séparation
Institut de Chimie Séparative de Marcoule
CEA, CNRS, ENSCM, Université de Montpellier
BP 17171, Marcoule, 30207 Bagnols-sur-Cèze (France)
E-mail: damien.bourgeois@umontpellier.fr
[b] M. M. R. y Morales, H. Dib, H. Kaper
Laboratoire de Synthèses et Fonctionnalisation des Céramiques Saint-Gobain Recherche Provence/CNRS, UMR 3080
550, Ave Alphonse Jauffret, 84306 Cavaillon (France)
E-mail: helena.kaper@saint-gobain.com
[c] J.-L. Rousset, F. Morfin, L. Burel
Université Claude Bernard Lyon 1
CNRS, IRCELYON
2, Ave Albert Einstein, 69626 Villeurbanne (France)

Supporting information for this article is available on the WWW under https://doi.org/10.1002/cctc.202300354

This publication is part of a Special Collection on "French Conference on Catalysis 2022". Please check the ChemCatChem homepage for more articles in the collection.

platinum supported on Al_2O_3 is used as catalyst for methane abatement.[12] Under oxidizing conditions, palladium usually shows the best performance among the platinum group metals,[13] leading to only CO_2 and water as products, making it an ideal model reaction for this study.

The presence of most palladium in e-waste arises from its use in multilayer ceramic capacitors (MLCCs).[14] Among the possible strategies employed for the reprocessing of e-waste, it has been evidenced that it is more suitable to process e-waste through sorting of components before shredding and grinding in order to recover palladium.[8b] Such sorting is generally performed after chemical or physical desoldering of components from printed circuit boards (PCBs).[15] The MLCCs used in the present study were provided from a recycling company (see experimental section). MLCCs are built of stacked ceramic layers of $BaTiO_3$ with the internal electrode composed of Ag and Pd in the form of a thin layer sandwiched between two $BaTiO_3$ layers. In previous studies dedicated to the recovery of Pd from e-waste, we demonstrated that Pd can be easily leached from those MLCCs after milling using an acidic aqueous solution.[8b] This approach appears to be the most efficient for Pd recovery from such waste as i) pyrometallurgy cannot be employed as the ceramic is refractory and the Cu content is too low in order to employ latter metal as a collector, ii) the Pd is alloyed with Ag, and diluted nitric acid is sufficient to leach all the Pd without complete leaching of the ceramic. We therefore focus on the best way to directly prepare an active Pd-catalyst from such leachates, employing and modifying metal deposition processes which have been classically employed for the preparation of Pd supported catalysts from aqueous solutions. The support used in the study is γ-Al_2O_3, a typical support used in heterogeneous catalysis due to its high surface area, chemical inertness and thermal stability.[16]

In the present paper, we propose to detail our investigations regarding the technical challenges associated with the approach in the field of methane oxidation, through straightforward preparation of a palladium-based heterogeneous catalyst, starting from real industrial waste, collected from electronics industry. The goal is not to develop new catalysts from a technology point of view, but to prepare and characterize palladium-based catalysts starting directly from e-waste, without isolation of palladium, and especially with no additional separation steps from other metals also contained in the waste. The challenge assessed in this study is to bridge the gap between a complex solution of metal cations arising from e-waste reprocessing, and catalyst preparation which is generally carried out from single-metal solutions of composition well mastered through the choice of suitable palladium salts. We thereby focus on the preparation of the catalysts using leaching of the waste in acidic medium and precipitation of the desired species (Pd) on the catalyst support (alumina). In particular, the role of impurities from the electronic waste (e.g. Ag, Ba, Bi, Ti) on the catalytic performance is studied on model solutions and real electronic waste.

Results and Discussion

Optimization of Pd leaching for catalyst preparation

The first objective assesed in this work is the leaching of the Pd contained in the MLCCs, targeting quantitative Pd recovery. The main elements composing the MLCCs are first qualitatively identified by energy dispersive X-ray spectroscopy used with scanning electron microscopy (SEM-EDS) analysis (Figure 1) and by semi-quantitative inductively coupled plasma-optical emission spectroscopy (semi-quantitative ICP–OES) analysis (Table S2). SEM analysis of a MLCC cross section visualizes the stacking of ceramic layers and internal electrodes (Figure 1a, 1b) and the SEM-EDS analysis displays the nature and the location of the different elements: the internal electrode is composed of Pd (b-1) and Ag (b-2), while the ceramic layers are

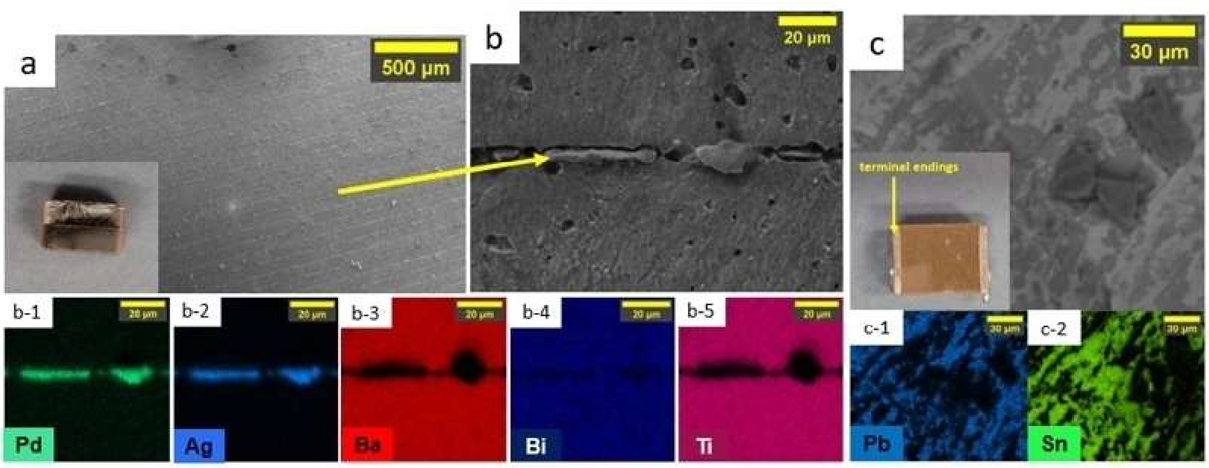

Figure 1. Qualitative elemental analysis of the MLCCs used in the study. (a), (b) Cross section of a MLCC at different magnifications and corresponding SEM-EDS analysis: turquoise: Pd (b-1), blue: Ag (b-2), red: Ba (b-3), dark blue: Bi (b-4) and pink: Ti (b-5). (c) SEM analysis of a MLCC terminal ending and SEM-EDS analysis showing other elements: Pb: blue (c-1) and Sn: green (c-2).

Research Article
doi.org/10.1002/cctc.202300354
Chemistry Europe
European Chemical Societies Publishing

composed of Ba (b-3), Ti (b-4) and Bi (b-5). SEM-EDS analysis of a terminal ending of a MLCC (Figure 1c) shows the presence of additional elements: Pb (c-1) and Sn (c-2), probably arising from solders. To precisely quantify the chemical composition of the MLCCs, ICP-OES analysis is performed on the solution obtained by complete digestion of crushed MLCCs. The heterogeneity of the starting material can lead to important error in the chemical quantification.[17] The experiment was repeated five times in order to estimate the error resulting from the sampling of the crushed MLCCs: the crushed material is relatively homogeneous when samples of 5 g or more are used for each experiment (Table S3). In all experiments using real e-waste, a minimum sample quantity of 5 g was thus employed. The MLCCs used in this study have a mean Pd content of 1.6 wt.%, with other major elements being Ba (40 wt.%), Ti (18 wt.%), Bi (6.9 wt.%) and Ag (4.6%); other elements such as Pb, Cu, Ni and Sn are present in smaller contents (Table 1). One challenge in using recycled Pd from leaching is to accomodate the leaching conditions, e.g. strong acidic conditions, and the impregnation method. As we aim to directly use the MLCCs acidic leaching solution as the impregnation medium, care has to be taken to preserve the support.

In our previous studies,[8b] the concentration of nitric acid was chosen according to the subsequent Pd separation stage using solvent extraction. Furthermore, the waste stream employed was of different origin than the one employed in the present study: waste PCBs collected from electronic devices, which also contained Cu and Fe. Here, we target to minimize the HNO_3 concentration while recovering a maximum of Pd with a maximum concentration in the leachate. The nature of the acid was not changed from our previous study, as it has already been evidenced that nitric acid is the best choice for a mineral acid to perform leaching of Pd–Ag alloys.[8b] Figure 2 shows the effect of varying the solid/liquid (S/L) ratio between crushed MLCCs and the volume of the HNO_3 solution and the effect of the HNO_3 concentration on the leaching yield of Pd and the other major elements present in the MLCCs. Figure 2a presents the effect of the S/L ratio on the Pd recovery yield. The S/L ratio variies between 272 $g.L^{-1}$ and 54.4 $g.L^{-1}$ by increasing the HNO_3 solution volume, while keeping the amount of milled MLCCS and HNO_3 concentration fixed (5.44 g of milled MLCCs, HNO_3 3 M). The corresponding range of solid loading variies between 272 $g.L^{-1}$ and 54.4 $g.L^{-1}$. The leaching efficiency of Pd does not change significantly relatively to the different S/L ratios with a slight maximum (96%) obtained with a 110 $g.L^{-1}$ S/L ratio, indicating that under these conditions, almost all Pd can be recovered. It is key to mention here that for S/L ratio lower or equal to 110 $g.L^{-1}$, no Pd is detected in the residual solid using SEM-EDS analysis. Thus, although there seems to be a tendency for a decrease in Pd leaching efficiency when using lower S/L ratio (higher leaching volume), we are not sure that this tendency is statistical relevant. There is no obvious reason for the leaching yield to decrease with decreasing solid/liquid ratio. Decreasing the S/L ratio leads on the other hand to higher Ba and Ti dissolution yield. The concentration of Ti and Ba in the leachate does not correlate

Table 1. Content (wt%) of principal metallic elements found in MLCCs.

Element	Pd	Ag	Ba	Bi	Ti	Pb	Cu	Ni	Sn
Content (wt%)[a]	1.6±0.05	4.6±0.2	40±0.8	6.9±0.6	18±0.7	1.0±0.1	0.35±0.01	0.10±0.01	0.1±0.05

[a] Determined by ICP-OES analysis.

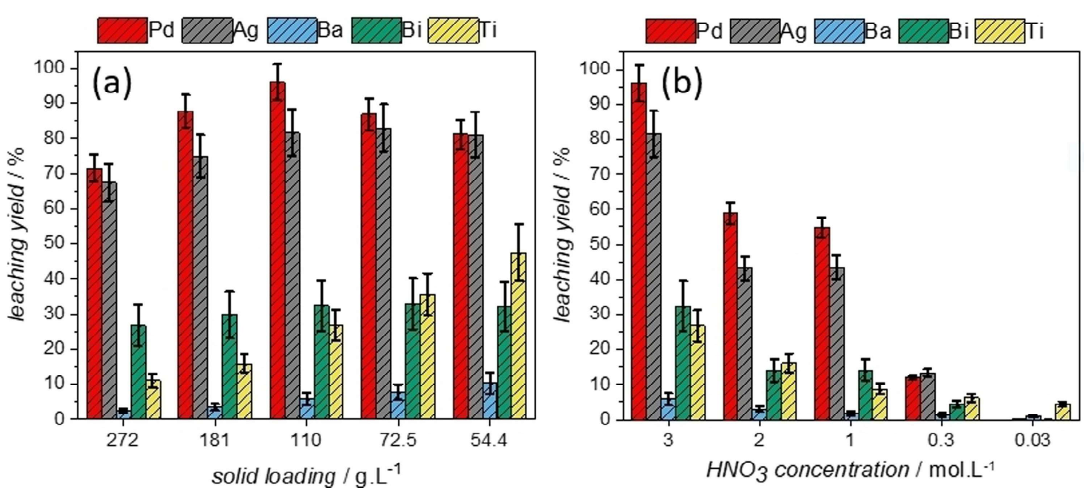

Figure 2. Results of the optimization of the leaching of Pd from milled MLCCs. Leaching yields of Pd and major impurities (a) as a function of the solid/liquid ratio between crushed MLCCs and a 3 M HNO_3 leaching solution of different volumes (3 M HNO_3 solution of 20–100 mL, 5.44 g of crushed MLCCs, 4 h, 80 °C) and (b) as a function of the HNO_3 concentration using a constant solid loading of 110 $g.L^{-1}$ (50 mL of HNO_3 solution, 5.44 g of crushed MLCCs, 4 h, 80 °C). The error bars correspond to the error from ICP analysis.

with the S/L ratio, and is limited to around 5 g.L^{-1} for Ti and 2.5 g.L^{-1} for Ba. This suggests that the leaching of these elements is limited by their solubility in the solution. For all three elements (Pd, Ti and Ba), there is a large excess in H^+ brought by the HNO_3: at least 50 fold for Pd, and 80 fold for Ba, based on the consumption of 2 H^+ per atom of metal to oxidize. Interestingly, the Ti/Ba molar ratio in the solution was always largely superior to 1 (between 3.1 and 6.3), indicating a noncongruent dissolution mechanism of the $BaTiO_3$ ceramic. This observation can be related to previous studies reporting the sorption of Ba^{2+} ions on the residual $BaTiO_3$ surface.[18] The Ti was not monitored in the study, so it is not possible to discuss the Ti/Ba molar ratio values obtained. Altogether, for this study, in order to limit the amount of Ti and Ba leached concomittantly to Pd, the leaching volume was set to 50 mL (110 g.L^{-1} solid/liquid ratio).

Second, as an excess of HNO_3 is required for the dissolution of Pd, the effect of the HNO_3 concentration on the recovery of Pd is studied using the optimized leachate volume with a solid loading of 110 g.L^{-1} (Figure 2b). The leaching efficiency of Pd decreases significantly by lowering the HNO_3 concentration from 3 M to 0.03 M. The major impurities (Ag, Ba, Bi, Ti) follow the same trend. As the objective is to recover maximum quantity of Pd, the leaching conditions are in the following set to a concentration of 3 M HNO_3 and 110 g.L^{-1} solid loading, although these conditions also give quite high concentration of major impurities. A representative composition of leachate obtained under these conditions is given in Table 2. Although Pd and Ag concentrations in the leachate are found relatively consistent (RSD below 5% on 5 replicates, Table S4), there can be an important variation in Ba, Ti and Bi concentrations (RSD between 17 and 30%, Table S4). This variation is attributed to the low dissolution yield of these elements and may arise from a global solubility limit, but was not further studied. As a consequence, when preparing catalysts from leachates prepared from real waste, the composition of the solution used is always indicated in order account for these variations.

Preparation and characterization of the catalysts

Starting from this Pd containing leachate, the objective is to prepare Pd supported on y-Al_2O_3 catalysts with a Pd loading of ca. 1 wt.%, thereby accomodating the conditions of acid leaching with optimum impregnation conditions. Indeed, the concentration of Pd in the obtained leachate is far too low to envision incipient wetness impregnation process. The preparation of supported catalyst using an acidic solution with such a concentration of 3 M HNO_3 is not conventional. When performing the preparation by wet impregnation, we observed that the strong acidity of the leachate impacts the crystal stability depending on the solid/liquid (S/L) separation process performed at the end of the impregnation. Preliminary experiments are carried out to prepare 1%Pd/y-Al_2O_3 with a solution containing $Pd(NO_3)_2$ precursor in 3 M HNO_3 using filtration and solvent evaporation as two classical techniques. When the S/L separation is performed by filtration, no Pd is deposited on the support. The y-Al_2O_3 support is strongly altered when performing the S/L separation by evaporation under reduced pressure, set in evidence by complete loss of the crystallinity of the support (Figure S1). As a result, conventional methods such as evaporation of the solvent or filtration[19] are not well adapted to the direct use of the MLCCs leachates. As a third route, we used the deposition-precipitation (DP) method. The DP method is more often employed for the preparation of gold catalysts,[20] and only few authors reported this method for the preparation of Pd-supported catalysts on ZrO_2[21] and CeO_2.[22] In a first attempt, the pH is raised to 10.5 using Na_2CO_3 as a base as reported for the preparation of bimetallic Pd–Fe/y-Al_2O_3 and Pd–Ni/y-Al_2O_3 catalysts[23] and monometallic Pd/ZrO_2 catalysts.[21] Then, the obtained suspension was subsequently filtered, washed, dried and calcined under air at 450 °C for 3 h (see experimental section). Under these conditions, a quantitative deposition of Pd onto the support while preserving its crystallinity is achieved and a 1.0 wt.% Pd catalyst is obtained (see Table 2). The obtained catalyst is denoted as DP10.5/Al_2O_3-r to indicate the deposition technique (DP), final pH (10.5) and origin of the palladium solution ("r" for real solution derived from MLCC leaching, and "m" for model solutions prepared from pure metal nitrates). Major impurities, i.e. Ag, Ba, Bi and Ti are also co-deposited quantitatively, and the composition of the catalyst directly reflects the composition of the leachate. To evaluate the impact of major impurities (Ag, Ba, Bi) on the catalytic performance, model polymetallic catalysts combining Pd with Ag, Ba and/or Bi are prepared and compared to a monometallic Pd/y-Al_2O_3 catalyst. The mass contents of the elements (wt%), the specific surface area (SSA) and the pore volume (V_{pore}) of the studied model Pd-based single metal and polymetallic catalysts and the catalyst derived from waste ("r") are listed in Table 3.

The powder X-ray diffraction patterns (XRD) of the catalysts prepared by the DP method are shown in Figure 3. All the XRD patterns show peaks belonging to y-Al_2O_3 (JCPDS # 00-050-0741) at 2Θ values at 19.4 (111), 32.5 (220), 37.4 (011), 39.3 (222), 45.8 (400), 60.7 (511) and 66.9° (440), indicating that the preparation method does not impact the crystal structure of the oxide support. Except for the Pd–Ag/Al_2O_3-m and the Pd–Ba/Al_2O_3-m catalysts, the XRD data of the different catalysts do not show reflection peaks for PdO, probably due to a high dispersion of the PdO particles and low weight loading (ca. 1 wt.%)l. The XRD diffraction patterns of the bi-metallic catalysts Pd–Ag/Al_2O_3-m reveal three diffraction peaks of metallic Ag (JCPDS # 04-0783) at 38.1°, 64.4° and 77.3° and two diffraction

Table 2. Elemental composition (mg.L^{-1}) of the MLCCs leachate and of the DP10.5/Al_2O_3-r catalyst (wt%) prepared via quantitative DP of the acid leachate on y-Al_2O_3 with a targeted loading in Pd of 1.00 wt.%.

Element	Pd	Ag	Ba	Bi	Ti	Pb	Cu, Ni, Sn
Acid leachate (mg.L^{-1})[a]	1690	4620	3600	2380	4900	350	< 100
DP10.5/Al_2O_3-r (wt%)[a]	1.0	2.8	2.2	1.4	3.0	0.2	< 0.1

[a] Determined by ICP-OES analysis.

Table 3. Weight loadings in Pd, Ag, Ba and Bi (wt%), specific surface area (SSA) and pore volume (V_{pore}) of the studied model catalysts and of the DP10.5/Al_2O_3-r catalyst. For the DP10.5/Al_2O_3-r catalyst only the weight loading of Pd, Ag, Ba and Bi are presented for clarity purpose (see Table 2 for the complete elemental composition).

	Pd loading (wt%)[a]	*Ag loading* (wt%)[a]	*Ba loading* (wt%)[a]	*Bi loading* (wt%)[a]	*SSA* ($m^2.g^{-1}$)[b]	V_{pore} ($cm^3.g^{-1}$)[b]
Pd/Al_2O_3-m	1.0	–	–	–	188	0.47
Pd–Ag/Al_2O_3-m	0.9	2.3	–	–	170	0.41
Pd–Ba/Al_2O_3-m	0.8	–	2.4	–	165	0.40
Pd–Bi/Al_2O_3-m	0.9	–	–	1.2	150	0.36
Pd–Ag–Ba–Bi/Al_2O_3-m	1.1	2.7	2.3	1.3	143	0.35
DP10.5/Al_2O_3-r	1.0	2.7	2.3	1.3	143	0.35

[a] Determined by ICP-OES analysis. [b] Determined by N_2 adsorption/desorption isotherms measurements. m indicates that the catalysts are obtained from model metal salt solutions, r indicates that the catalyst is obtained from the leachate of MLCCs.

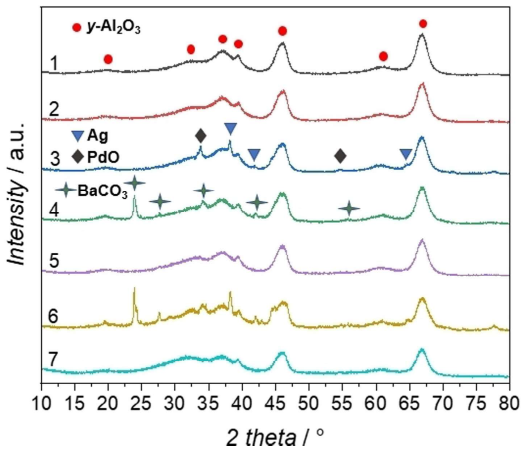

Figure 3. Diffractograms of the oxide support (1) y-Al_2O_3 and model catalysys (2) Pd/Al_2O_3-m, (3) Pd–Ag/Al_2O_3-m, (4) Pd–Ba/Al_2O_3-m, (5) Pd–Bi/Al_2O_3-m and (6) Pd–Ag–Ba–Bi/Al_2O_3-m, and of catalyst prepared using the MLCCs leachate (7) DP10.5/Al_2O_3-r.

peaks that are characteristic of PdO (JCPDS # 41–1107) at 33.8° and 54.7°. The presence of PdO is confirmed by the disappearance of the two associated peaks after reduction of the catalyst under H_2 flow before performing the XRD analysis (Figure S2). Careful analysis of the Pd–Ag/Al_2O_3-m diffraction pattern do not allow identifying whether Ag and Pd form an alloyed nanomaterial or a mixture of monometallic Ag and Pd particles.[24] The XRD pattern of the bi-metallic Pd–Ba/Al_2O_3-m catalyst shows characteristic peaks of $BaCO_3$ (JCPDS # 44–1487) at 24.0°, 27.7°, 34.2°, 41.9° and 55.7°. The catalyst Pd–Ag–Ba–Bi/Al_2O_3-m seems to show a combination of the additional peaks observed on the Pd–Ag/Al_2O_3-m and Pd–Ba/Al_2O_3-m catalysts, however given the number of metals on the surface, their precise identification is not straightforward.

The distribution of Pd and the impurities on the catalyst surface is of peculiar interest for this study, since the impurities might play an important role on the overall catalytic performance. First, we look at the Pd particle size distribution using HAADF-STEM analysis after a reductive treatment (200 °C under H_2 during 1 h), representative of the reduction carried out before the CH_4 catalytic oxidation tests. A representative microphotograph of Pd/Al_2O_3-m observed by HAADF-STEM and the lognormal particle size distribution are shown in Figure 4. The Pd/Al_2O_3-m monometallic catalyst demonstrates a uniform distribution of small spherical metal particles over the support surface, their diameter varies between 1.6 to 4.2 nm, and the average diameter is 2.7+/−0.6 nm, which is in good accordance with the XRD data.

The catalysts are further analyzed using transmission electron microscopy coupled with EDS (TEM-EDS) to visualize the distribution of Pd and impurities on the surface. The Pd–Ba/Al_2O_3-m catalyst shows distinctive spherical Pd particles with a size of 3–5 nm on the surface (Figure S3) in addition to large mixed bimetallic Pd–Ba agglomerates. In contrast to Pd/Al_2O_3-m and Pd–Ba/Al_2O_3-m, Pd–Ag/Al_2O_3-m catalyst does not show isolated Pd nanoparticles, only Pd–Ag bimetallic particles of 4–11 nm or aggregates of 35–160 nm are observed on the support surface (Figure S4). The study of Pd–Ag/Al_2O_3-m and Pd–Ba/Al_2O_3-m catalysts by TEM-EDS suggests that the agregation or mixing of Pd with Ag is more favorable than with Ba, leading to isolated Pd nanoparticles in the case of Pd–Ba/Al_2O_3-m catalyst. Indeed, it is well reported in the literature that Pd and Ag form stable alloys.[25] To the best of our knowledge, only few studies report the preparation of palladium-based bimetallic catalysts using a deposition-precipitation method. Incipient wetness co-impregnation or sequential impregnation are widely reported in the literature and allow obtaining a more uniform composition of the bimetallic particles across the support

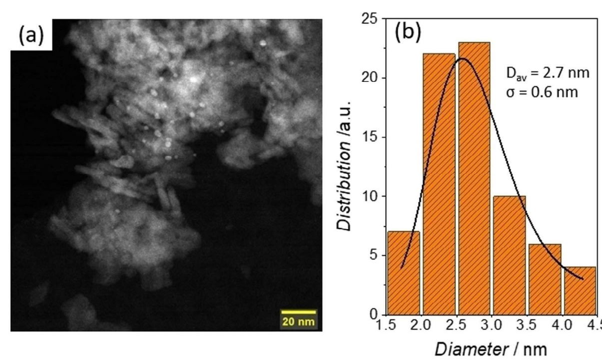

Figure 4. Microstructural analysis of the monometallic Pd/Al_2O_3-m catalyst. (a) HAADF-STEM microphotograph and (b) corresponding lognormal size distribution of the Pd nanoparticles.

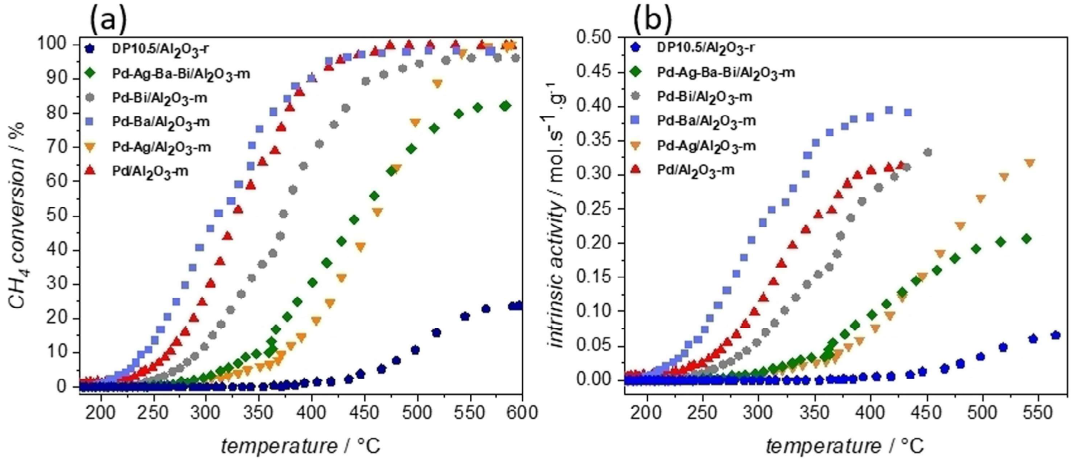

Figure 5. (a) Methane conversion as a function of the reaction temperature for the studied catalysts. (b) Intrinsic activies of the studied catalysts as a function of the reaction temperature. Reaction conditions : U-shaped fixed bed reactor, CH_4: 2000 ppm, O_2: 10'000 ppm, heating rate : 3 °C.min^{-1}, GHSV = 10'000 h^{-1}.

surface. For these methods it is well established that the formation of polymetallic species and thus their distribution on the support surface does not take place during the impregnation or the deposition step but during the thermal or reductive treatment.[26] When looking at the catalyst prepared from real waste using HAADF-STEM coupled with EDS (HAADF-STEM-EDS), we also do not observe isolated Pd particles, similar to the Pd–Ag/Al_2O_3-m catalyst (Figure S5). The surface is covered by two species: Ag nanoparticles and aggregates of particles with various atomic ratios of Pd, Ag, Bi, Ti. Even though EDS is a semi-quantitative method, and the chemical composition of the aggregates should be interpretated with care, it appears that within these aggregates, Pd represents the lower fraction of metals present. The result corresponds roughly to the initial composition of the catalyst, with a Pd:Ag ratio of 1:2.25 (Pd:Ag in the catalyst: 1:2.8, see Table 2). The lower ratio in the aggregates can be explained by the fact that some Ag is present as isolated particles. The analysis of this catalyst also demonstrates the difficulty when working with secondary raw materials such as electronic waste. It is not evident to analyze the catalyst surface using standard techniques due to the impurities.

CH_4 catalytic oxidation tests

To evaluate the feasibility to directly valorize the MLCCs leachate without purification, the impact of major impurities (Ag, Ba, Bi) on the catalytic performance is studied in the following. The conversion of CH_4 as a function of the reaction temperature for the model studied monometallic catalyst Pd/Al_2O_3-m, multi-metallic catalysts Pd–Ag/y-Al_2O_3-m, Pd/Ba/y–Al_2O_3-m, Pd/Bi/y-Al_2O_3-m, Pd/Ag/Ba/Bi/y-Al_2O_3-m and for the DP10.5/Al_2O_3-r catalyst is presented in Figure 5 (a). Since the studied catalysts have slight variations in their Pd loading, catalyst performances are also presented in terms of intrinsic activity (r, expressed in mol.s^{-1}.g^{-1} of Pd). The intrinsic activities of the studied catalysts as a function of reaction temperature, for temperature ranging from 180 to 550 °C are plotted in Figure 5 (b). The catalytic performances in terms of conversion and intrinsic activity are compared considering the third cycle upon decreasing the temperature. The preparation of a Pd supported on alumina catalyst using directly the MLCCs leaching solution (DP10.5/Al_2O_3-r) leads to the co-deposition of impurities present in the leachate (mainly Ag, Bi, Ba and Ti) with non-negligible loadings (see Table 2). Although the targeted Pd loading was effectively deposited on the DP10.5/Al_2O_3-r catalyst, its catalytic performance is very low compared to the monometallic catalyst Pd/Al_2O_3-m. Since they are prepared following the same experimental conditions, this dramatic decrease in the catalytic performance can be attributed to the presence of the co-deposited impurities on the DP10.5/Al_2O_3-r catalyst. Therefore catalytic tests are performed on the model polymetallic catalyst to figure out the effect of major impurities (Ag, Bi, Ba). The single metal Pd/Al_2O_3-m catalyst shows similar catalytic performances as previously reported elsewhere,[27] which validates that the DP method can be used to prepare Pd–Al_2O_3 catalysts under the studied conditions. Even better oxidation activity is observed for the Pd–Ba/Al_2O_3-m catalyst. The temperature corresponding to 10% (T_{10}) and 50% (T_{50}) methane conversion is 22 °C lower for Pd–Ba/Al_2O_3-m than for the monometallic Pd/Al_2O_3-m catalyst (Table 4).

This result is not surprising since it was already reported that the addition of Ba to Pd/Al_2O_3 catalysts improves the catalytic activity for CH_4 oxidation by increasing the electron density on the active metal surface, which weakens the adsorption strengh of hydrocarbons on Pd.[28] It can be clearly seen from all the model bimetallic catalysts that Ag as impurity has the strongest negative impact on the catalytic performance compared to the Pd/Al_2O_3-m catalyst with an increase of T_{10} by 103 °C and T_{50} by 132 °C compared to Pd/Al_2O_3-m (see Table 4). The significant decrease in activity between Pd–Ba/Al_2O_3-m and

Research Article
doi.org/10.1002/cctc.202300354

Table 4. Highest conversion obtained, temperature corresponding to 10% (T_{10}) and 50% (T_{50}) CH_4 conversion and highest intrinsic activity ($mmol.s^{-1}.g^{-1}$ of Pd) of the studied catalysts.

Catalyst	X_{max} (%)	T_{10} (°C)	T_{50} (°C)	Intrinsic activity T (°C)[a]	r_{max} ($mmol.s^{-1}.g^{-1}$ of Pd)
Pd/Al_2O_3-m	100	265	328	427	312
Pd–Ag/Al_2O_3-m	100	373	460	542	318
Pd–Ba/Al_2O_3-m	100	244	306	417	395
Pd–Bi/Al_2O_3-m	100	292	372	451	332
Pd–Ag–Ba–Bi/Al_2O_3-m	83	349	443	539	207
DP10.5/Al_2O_3–r	24	493	-	600	65

[a] Corresponding temperature for the highest intrinsic activity.

Pd–Ag/Al_2O_3-m cannot be explained by their SSA and pore volumes since they are very similar (see Table 3). TEM-EDS analysis of the Pd–Ba/Al_2O_3-m catalyst shows isolated Pd nanoparticles with a size of 3–5 nm, whereas no isolated Pd particles are found on the Pd–Ag/Al_2O_3-m catalyst. This suggests that the specific agregation of Pd and Ag, which does not allow the formation of isolated Pd particles, decreases the catalytic performance of Pd–Ag/Al_2O_3-m. Although bimetallic Pd–Ag catalysts are widely reported in the literature for acetylene selective hydrogenation,[25b,26b] to the best of our knowledge only one paper reports the performance of bimetallic Pd–Ag supported on alumina catalyst for methane total oxidation.[29] The authors demonstrate that a Pd–Ag bimetallic catalyst with 3:1 molar ratio of Pd:Ag prepared by incipient wetness impregnation gives either similar or even better catalytic performances than a monometallic 1%Pd/Al_2O_3 catalyst depending on the O_2/CH_4 ratio. This is in contradiction with our results for the Pd–Ag/Al_2O_3-m catalyst and the reasons could arise from *(i)* the different preparation method, *(ii)* the difference in the Pd:Ag molar ratio corresponding to 1.0:2.3 in this study. This suggests that the impact of Ag on the catalytic performance may strongly depend on the Pd:Ag ratio, and thus on the relative concentration of Pd and Ag in the leaching solution. The bimetallic Pd–Bi/Al_2O_3-m has a smaller impact on the catalytic performance than the Pd–Ag/Al_2O_3-m catalyst with an increase of the T_{10} by 27 °C and T_{50} by 44 °C compared to the monometallic Pd/Al_2O_3-m catalyst (see Table 4). In this context it is interesting to note that the ratio of Pd:Bi is 1.0:0.6, which might explain the better performance of the Bi-containting catalyst compared to the Pd–Ag catalyst, since the shielding of Pd by the Bi is lower.

The most significant result is the drop in performance when going from model catalysts to the catalyst prepared using directly the MLCCs leaching solution. Indeed, the activity of the catalyst derived from MLCCs leaching is very low, with a T_{10} of 493 °C compared to 265 °C for Pd/Al_2O_3-m and an intrinsic activity of 65 $mmol.s^{-1}.g^{-1}$ at 600 °C. To understand this difference, a model catalyst including all the major impurities is prepared, Pd–Ag–Ba–Bi/Al_2O_3-m. At low temperatures (below 360 °C) its performance is higher than the bimetallic Pd–Ag/Al_2O_3-m catalyst (Figure 5 a). Considering the fact that the Pd loading is slightly higher on the Pd–Ag–Ba–Bi/Al_2O_3-m catalyst, it is more reasonable to compare their relative performances in terms of their intrinsic activities (see Figure 5 (b)). Above 450 °C, the slope of the Pd–Ag/Al_2O_3-m catalyst is significatively higher than the Pd–Ag–Ba–Bi/Al_2O_3-m catalyst with a maximal activity at approximately 542 °C of 318 $mmol.s^{-1}.g_{Pd}^{-1}$ for the bimetallic Pd–Ag catalyst and of 207 $mmol.s^{-1}.g_{Pd}^{-1}$ for the Pd–Ag–Ba–Bi/Al_2O_3-m catalyst. Therefore, Pd–Ag–Ba–Bi/Al_2O_3-m shows the strongest decline in the catalytic performance. Again, no isolated Pd particles can be observed on the Pd–Ag–Ba–Bi/Al_2O_3-m catalyst, showing that the impurities shield the Pd and thus render the catalyst inactive. Another difference between the model and real catalyst is the presence of Ti as an additional impurity in DP10.5/Al_2O_3-r with a Ti-loading of 2.7 wt.%.

The impregnation protocole is therefore optimized with the aim to precipitate Pd before Ag when the base Na_2CO_3 is added during the preparation of the catalyst. The fraction (%) of Pd and major impurities (Ag, Ba, Bi) deposited on the y–Al_2O_3 support from a model solution containing Pd, Ag, Ba and Bi as a function of the pH during precipitation is presented in Figure 6. At a pH of 4.0, 100% of the Pd in the impregnation solution was deposited on the y-Al_2O_3 support while only

20% of Ag was co-deposited. At this specific pH, 100% of Bi and less than 10% of Ba are also co-deposited. The experiment

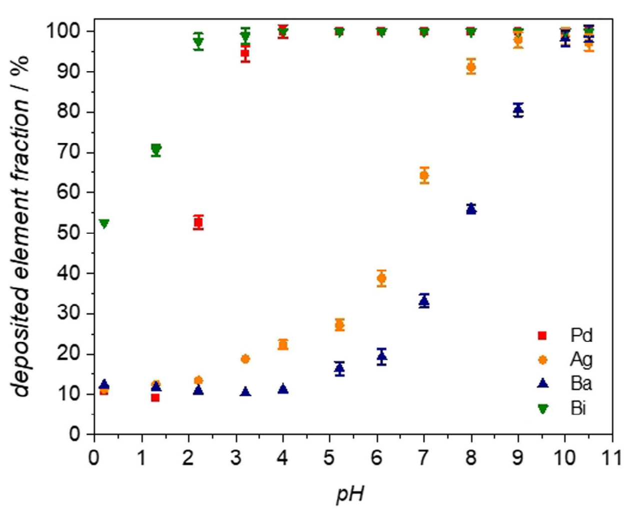

Figure 6. Fraction (%) of Pd and major impurities (Ag, Ba, Bi) deposited on the y–Al_2O_3 support as a function of the pH during the DP with Na_2CO_3.

is performed on a model solution which does not contain Ti as all our attempts to prepare an aqueous solution of Ti^{4+} and Pd^{2+} failed. This is not surprising as Ti^{4+} is well known for rapid hydrolysis, even at very low pH.[30] Furthermore, a previous study on selective precipitation of Ti from acidic sulfate solutions revealed quantitative precipitation of Ti upon increasing the pH between ph 2.5 and pH 3.0.[31] Based on this, a catalyst using directly the MLCCs leaching solution is prepared by DP with addition of Na_2CO_3 at pH = 4.0. The elemental loadings (wt%) of the prepared catalyst (DP4/Al_2O_3-r) are presented in Table 5. While Ag in the MLCCs leaching solution is quantitatively deposited on the y-Al_2O_3 support when raising the pH to 10.5 (see Table 2), only 36% of Ag is deposited at pH = 4.0 (Table 5). Also, only 27% of Ba is deposited at pH = 4.0, while Pd, Bi and Ti are deposited quantitatively. The change in the final pH from 10.5 to 4 does not impact the crystallinity of the *y*-Al_2O_3 support and the DP4/Al_2O_3-r catalyst shows the same diffractogram as the DP10.5/Al_2O_3-r catalyst with characteristic peaks of the *y*-Al_2O_3 support (Figure S7). Also, a model catalyst with only Pd prepared at pH = 4 shows the same catalytic performance as the Pd/Al_2O_3-m prepared at pH = 10.5, demonstrating that the change in pH does not impact the active Pd-phase (results not shown here).

The conversion of CH_4 and the intrinsic activity as a function of the reaction temperature for the DP4/Al_2O_3-r are presented

Table 5. Elemental composition (mg.L^{-1}) of the MLCCs leachate used for the preparation of the DP4/Al_2O_3-r catalyst via DP up to a pH of 4 with a targeted loading in Pd of 1.00 wt.% and metallic loadings on the catalyst (wt%).

Wt%	Pd	Ag	Ba	Bi	Ti	Pb	Cu	Ni, Sn
Acid leachate (mg.L^{-1})[a]	1683	4634	2512	3631	3063	531	630	< 100
DP4/Al_2O_3-r (wt%)[a]	1.0	1.0	0.4	2.2	1.9	0.3	0.1	< LD[b]

[a] Determined by ICP-OES analysis. [b] Limit of detection.

Table 6. Highest conversion obtained, temperature corresponding to 10% (T_{10}) and 50% (T_{50}) CH_4 conversion and highest intrinsic activity (mmol.s^{-1}.g^{-1} of Pd) for the DP4/Al_2O_3-r catalyst.

Catalyst	X_{max} (%)	T_{10} (°C)	T_{50} (°C)	Intrinsic activity T (°C)[a]	r_{max} (mmol.s^{-1}.g^{-1} of Pd)
DP4/Al_2O_3-r	100	334	411	518	313

[a] Corresponding temperature for the highest intrinsic activity.

in Figure 7 (a–b). A significant enhancement of the catalytic performance is observed compared to the catalytic performance of the DP10.5/Al_2O_3-r catalyst, confirming the undesirable impact of Ag on the catalytic performance.

The diminution of the Ag:Pd ratio to a 1:1 ratio gives an even better performance than the model multimetallic Pd–Ag–Ba–Bi/Al_2O_3-m catalyst with a relative decrease of the T_{10} by 15 °C and the T_{50} by 32 °C (Table 6), despite the presence of Ti- and Pb as additional impurities. Unlike the DP10.5/Al_2O_3-r catalyst, the analysis of the DP4/Al_2O_3-r using HAADF-STEM-EDS shows isolated Pd nanoparticles. Again, also aggregates of particles with various atomic ratios of Pd, Ag, Bi and Ti are observed, but compared to DP10.5/Al_2O_3-r, the aggregates contain more Pd relatively to other metals and this could explain the better catalytic performance of the DP4/Al_2O_3-r catalyst (Figure S6). Even though the catalytic performance of the DP4/Al_2O_3-r catalyst is still lower than the bimetallic Pd–Bi/Al_2O_3-m and the monometallic Pd/Al_2O_3-m catalyst, a significant improvement can be obtained by lowering the amount of impurities (and the presence of Ag in particular) by adjusting the pH during the precipitation. Although the direct impact of Ti impurity is not studied on a model catalyst, the better performance obtained with the DP4/Al_2O_3-r compared to the Pd–Ag–Ba–Bi/Al_2O_3-m catalyst suggests that Ti impurity has not a significative impact on the catalytic performance.

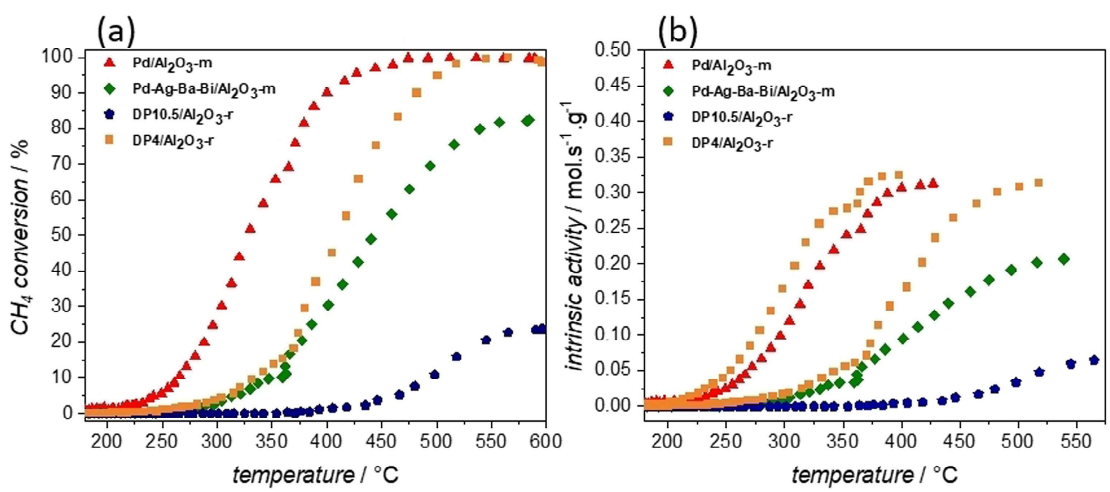

Figure 7. (a) Methane conversion and (b) intrinsic activies as a function of the reaction temperature for Pd/Al_2O_3-m, Pd–Ag–Ba–Bi/Al_2O_3-m, DP10.5/Al_2O_3-r and DP4/Al_2O_3-m. Reaction conditions : U-shaped fixed bed reactor, CH_4 : 2000 ppm, O_2 : 10'000 ppm, heating rate : 3 °C.min^{-1}, GHSV = 10'000 h^{-1}.

Conclusions

In this study, we started from a batch of MLCCs recovered from e-waste to prepare an active Pd-based catalyst for methane oxidation. One important aspect is to combine the technical solution for the leaching of Pd from waste, e.g. strong acidic media, with current impregnation methods to deposit Pd on a support (γ–Al_2O_3 in this study), thereby limiting the number of preparation steps. Thus, the leachate should directly serve as an impregnation media. The optimal leaching conditions from MLCCs is 3 M HNO_3 with a solid loading of 110 g.L^{-1}. The preparation of a heterogeneous catalyst is not straightforward, as the acidity of the solution risks to deteriorate the catalyst support, and the Pd concentration is too low to use incipient wetness impregnation. A suitable alternative presented here is the deposition-precipitation technique by increasing the pH of the leachate in the presence of the support. This technique is rather unconventional for the prepartion of Pd-based catalysts for methane oxidation. At pH 10.5, complete precipitation of Pd on γ–Al_2O_3 is obtained with a Pd particle size of 2–3 nm. However, impurities present in the leachate such as Ba, Bi and Ag are also deposited. In order to study the impact of these impurities on the catalytic performance, model catalysts using the same DP technique were prepared. Compared to bare Pd/Al_2O_3, the impurities lower the catalytic performance, especially for Ag as second metal. TEM analysis shows that the silver completely shields the Pd nanoparticles, and compared to Bi or Ba as impurities, no isolated Pd particles are present. For methane oxidation, excess Ag in Ag–Pd bimetallic catalysts lowers the catalytic performance. Furthermore, the performance of the catalyst derived from a real MLCC leachate is much lower than the model catalysts, despite a similar Pd loading. The impregnation protocole was therefore further optimized to reduce the impurity loading and optimize the Pd:impurities ratio. Indeed, at pH = 4, Pd is already deposited quantitively, while the amount of impurities can be significantly lowered. The catalyst prepared at pH = 4 shows better performance in methane oxidation than the one prepared at pH = 10, indicating the negative impact of a high impurity loading close to the active Pd species. Overall, our approach demonstrates that i) Pd recovered from electronic waste can be employed directly from the leachate, but the quality of the catalytic performance can be lowered in the presence of impurities, ii) some metals lower the catalytic performance, for either chemical and physical reasons (sheltering of Pd), and iii) some metals (eg. Ba) have no peculiar effect and can be easily tolerated. Further studies will be carried out to study the impact of purification on the depositions and catalytic performance.

Experimental Section

Materials

MLCCs sourcing: the MLCCs were supplied by a SOVAMEP, Muret, France, and about 1 kg of raw MLCCs were provided for the study. The MLCCs were crushed to a particle size < 200 μm by using a vibratory disc mill (Retsch RS 200). Nitric acid (HNO_3, 69.5 %) and hydrochloric acid (HCl, 37 %) were purchased from Carlo Erba. Barium carbonate ($BaCO_3$, ≥ 99 %) and bismuth(III) nitrate pentahydrate ($Bi(NO_3)_3$. ·5H_2O, ≥ 99.99 %) were purchased from Sigma Aldrich. Silver nitrate ($AgNO_3$, ≥ 99.0 %) was purchased from Merck. Palladium (II) nitrate hexahydrate ($Pd(NO_3)_2$. ·6H_2O, 99.9 %) and sodium carbonate anhydrous (Na_2CO_3, 99.5 + %) were purchased from STREM Chemicals. High purity de-ionized water (resistivity 18.2 mΩ cm) was obtained by means of a Milli-Q water purification system (Millipore) and was used throughout all the experiments.

Analytical techniques

For all the experiments, determination of metal concentrations were quantified by inductively coupled plasma optical-emission spectrometry (ICP–OES) on a Thermo Scientific iCAP 7400 series instrument. The detailed characterization procedures are described in the Supporting information. For MLCCs leaching solutions and precursors containing solutions for impregnation, aliquots were directly colected in triplicates and were diluted into a 1.0 % (w/w) HCl/HNO_3 aqueous solution with HNO_3/HCl = 9 (v/v) for the quantification of Pd, Ba, Sn, Ti, Al and into 1.0 % HNO_3 aqueous solution for the quantification of Na, Cu, Ni, Ag, Pb and Bi. For leaching residues and catalysts, 40.0 mg of the material were weighed and were subjected to microwave acid digestion (ETHOS UP, Milestone, Italy) at 210 °C in 5 mL of aqua regia (for further ICP-OES analysis of Pd, Ba, Bi, Ti, Pb, Cu, Ni, Sn, Nd elements) or in 5 mL of concentrated HNO_3 (for further ICP-OES analysis of Ag and Cu elements). Resulting solution were diluted with de-ionized water in a 20 mL volumetric flask and aliquots were collected in triplicates and were subjected to an appropriate dilution in 1.0 % (w/w) HCl/HNO_3 with HNO_3/HCl = 9 (v/v) and in 1.0 % (w/w) HNO_3. Semi-quantitative analysis of the MLCCs leaching solution was perfomed by ICP–OES on a Thermo Scientific iCAP PRO XP. Elemental chemical mappings of MLCCs cross sections and terminal endings were obtained by means of scanning electron microscopy (SEM) using a thermoionic SEM Tescan Vega microscope equipped with an energy dispersive spectrometer (Brucker EDS detector). The images were obtained at varied magnifications by applying accelerating voltage of 30 kV. The crystal structure of the Pd supported catalysts were characterized by means of the X-ray diffraction (XRD) technique on a Brucker D8 Endeavor diffractometer operating with a Cu Kα radiation source (40 kV, 40 mA) and nickel filter (λ = 0.15406 nm). The diffraction scans were taken within a 2Θ zone of 10 to 80° with a step of 0.01° and a scanning rate of 0.03°.s^{-1}. The diffractograms were qualitatively analyzed by using the EVA software package and the ICDD 2016 dabatase. Nitrogen (N_2) adsorption/desorption isotherms were acquired at 77 K with a Micromeritics tristar II 3020 instrument. Before analysis, catalysts were degassed under vacuum at 280 °C for 6 h. The specific surface areas (SSA) was calculated using the Brunauer-Emmet-Teller theory (BET) and pore volume (V_{pore}) was determined from the desorption branch of the isotherms using the Barrett-Joyner-Halenda (BJH) method.[32] The morphology, particle size distribution and local chemical composition of metal species supported on the catalysts were determined by transmission electron microscopy (TEM) and energy dispersive spectrometry (EDS). We used a JEOL 2100F (JEOL, Japan) microscope with a field emission gun (Schottky field emitter) operating at 200 kV. The high-angle annular dark-field STEM experiments (HAADF-STEM) were performed with a FEI Titan ETEM G2 electron microscope equipped with a Cs image aberration corrector and operated at 300keV.

Palladium leaching from MLCCs

To study the leaching of the MLCCs, i.e. the effect of HNO_3 concentration and volume on the leaching efficiency of Pd and other elements presents in the MLCCs, 5.44 mg of crushed MLCCs were weighed and placed into a round-bottom flask (50, 100 or 250 mL). An aqueous solution of HNO_3 (3–0.03 M) with volume ranging from 20 to 100 mL (See section 2.1) was then added and the round bottom flask was fitted with a Vigreux column. The solution was stirred (450 rpm) at 80 °C during 4 h using an IKA RCT magnetic stirrer and an oval PTFE magnetic stirrer bar. The resulting leaching solution, initially grey, turned to yellow and after decanting, a white residue was formed at the bottom of the flask. The leaching solution was first filtered on a Büchner funnel with a qualitative filter paper (grade 413), and then with a 0.45 μm syringe filter to remove fine particles. Total contents (wt %) of elements presents in the MLCCs were determined by the leaching of 5.44 g of crushed MLCCs in 50 mL of 3 M HNO_3 (4 h, 80 °C, 450 rpm) and by digestion of the resulting leaching residue. Each elements in the leaching solution and in the residue were quantified by means of ICP-OES and the elemental content was calculated using Equation (1):

$$Content\ (wt\%) = \frac{m_{LS} + m_{RD}}{m_{MLCCs}} \times 100 \qquad (1)$$

where mL_S is the dissolved amount of the element in the leaching solution (mg), m_{RD} is the dissolved amount from the residue digestion and m_{MLCCs} is the imput of crushed MLCCs in the leaching solution.

Catalyst preparation

The alumina (γ-Al_2O_3) used for the catalysts preparation was prepared by thermal decomposition in a muffle oven (Nabertherm) of a boehmite powder (Dispal 23-N4-80, Sasol) in ambiant atmosphere at 873 K for 24 h (heating ramp of 5 K.min^{-1}). The model catalysts, i.e. the catalysts prepared from a freshly made precursors containing solution, were denoted with the suffix -m as Pd/Al_2O_3-m, Pd–Ba/Al_2O_3-m, Pd–Ag/Al_2O_3-m, Pd–Bi/Al_2O_3- m and Pd–Ag–Ba–Bi/Al_2O_3-m, indicating the nature of metals supported on the γ–Al_2O_3 support. Pd-catalysts directly prepared from real leachate of MLCCs were denoted with the suffix-r as DP10.5/Al_2O_3-r and DP4/Al_2O_3-r, indicating the specific final pH reached during the impregnation. The model Pd based catalysts were prepared by a deposition-precipitation method (DP). Briefly, the appropriate Pd, Ag, Ba, Bi precursors were dissolved in a 3 M HNO_3 aqueous solution and the alumina powder was then added. Subsequently, the pH was raised to a value of 10.5 by the slow addition of a 1 M Na_2CO_3 aqueous solution. For all the model catalysts, the alumina powder was impregnated with pre-determined precursors concentrations : $Pd(NO_3)_2$ (0.426 %; w/v), $AgNO_3$ (0.724 %; w:v), $BaCO_3$ (0.517 %; w/v), $Bi(NO_3)_3$ (0.557 %, w/v) and the ratio of alumina powder to the impregnation solution was always maintained at 15.2 % (w/w) to reach a targeted weight loading of Pd of 1.0 % (w/w). For the catalysts prepared by using directly the MLCCs leachate, the alumina powder was directly added to the leachate and the pH was raised to 10.5 for DP10.5/Al_2O_3-r and to 4 for DP4/Al_2O_3-r. The ratio of alumina to the leachate was also adapted to obtain a targeted weight loading of 1.0 % for Pd. For all the catalysts, the obtained suspensions were subsequently filtered and washed with 50 mL of de-ionized water and the resulting solids were dried at 90 °C overnight and calcined in a tube furnace (Nabertherm) under dynamic air flow (20 L.h^{-1}) at 450 °C for 3 h (heating ramp of 2 °C.min^{-1}).

Catalytic activity evaluation

Methane combustion performances were carried out in a continuous flow fixed-bed setup equipped with a quartz U-shaped reactor and a furnace. 100 mg of the catalyst sample sieved between 125 and 250 μm was diluted with 100 mg of SiC to minimize the effect of hot spots. Prior to performing catalytic tests, a reduction of each sample was conducted under a hydrogen gas stream (40 % H_2/He) at 200 °C for 1 h. The methane combustion tests were performed under non-stoichiometric conditions (excess oxygen) : 2000 ppm of CH_4, 10,000 ppm of O_2 and He balance at the total flow rate of 10 L.h^{-1} corresponding to the gas hourly space velocity (GHSV) of 100,000 h^{-1} and at atmospheric pressure. Temperature was increased and decreased linearly up and down between 180 and 600 °C with a plateau of 30 min at 600 °C. This was repeated three times, i.e. three cycles were performed. The effluent gas was analyzed by a micro-gas chromatography instrument (SRA R3000) equipped with two capillary columns (MolSieve5 A PLOT, column PLOT U) and coupled with a thermal conductivity detector (TCD). The rate of CH_4 conversion (X CH_4) was calculated using Equation (2):

$$X\ CH_{4\ (g)}(\%) = \frac{CH_{4\ (g)\ in} - CH_{4\ (g)\ out}}{CH_{4\ (g)\ in}} \times 100 \qquad (2)$$

where $CH_{4\ (g)\ in}$ is the initial concentration of CH_4 and $CH_{4\ (g)\ out}$ is the concentration at a given temperature.

Intrinsic catytic activity of CH_4 transformation, r, (expressed in mol.s^{-1}.g^{-1} of Pd) was calculated following Equation (3):

$$r\ (mol.s^{-1}.g^{-1}\ of\ Pd) = Q\frac{1}{V_{mol}}\ \frac{273}{T_{exp}}\ \frac{CH_{4\ (g)\ in}}{10^6}\ \frac{1}{m_{cata}}\ \frac{X_{CH_4}}{\%_{Pd}} \qquad (3)$$

where Q is the total gas flow rate (L.s^{-1}), V_{mol} = 22.4 L.mol^{-1}, $CH_{4\ (g)\ in}$ in is the initial CH_4 concentration (ppm), $X\ CH_4$ is the CH_4 conversion (%), T_{exp} is the analysis temperature (K), m_{cata} is the catalyst mass (g), $\%_{Pd}$ is the weight loading of Pd in the catalyst (%).

Acknowledgements

The authors are grateful to the Agence Nationale de la Recherche (ANR) for funding of the study (Projet ANR–21–CE07–0057–01) and to the Région Occitanie and Saint-Gobain Research for funding the PhD thesis grant of MMRM. We would also like to thank Béatrice Baus-Lagarde for kind help during the ICP-OES analysis.

Conflict of Interests

The authors declare no conflict of interest.

Data Availability Statement

The data that support the findings of this study are available from the corresponding author upon reasonable request.

Chemistry Europe
European Chemical Societies Publishing

Keywords: catalyst preparation · e-waste recycling · methane oxidation · palladium · polymetallic catalysts

[1] L. Bloxham, S. Brown, L. Cole, A. Cowley, M. Fujita, N. Girardot, J. Jiang, R. Raithatha, M. Ryan, B. Tang, A. Wang, *Johnson Matthey Technology Review* **2022**.
[2] M. Delporte, J. Cavailles, M. Martin Romo y Morales, N. Bion, L. Nodari, X. Courtois, F. Can, H. Kaper, *Inorg. Chem.* **2022**, *61*, 15432–15443.
[3] H. U. Sverdrup, K. V. Ragnarsdottir, *RCR* **2016**, *114*, 130–152.
[4] a) A. Işıldar, E. R. Rene, E. D. van Hullebusch, P. N. L. Lens, *RCR* **2018**, *135*, 296–312; b) Y. Ding, S. Zhang, B. Liu, H. Zheng, C.-C. Chang, C. Ekberg, *RCR* **2019**, *141*, 284–298.
[5] Z. Sun, Y. Xiao, H. Agterhuis, J. Sietsma, Y. Yang, *J. Clean Prod.* **2016**, *112*, 2977–2987.
[6] a) H. Li, J. Eksteen, E. Oraby, *RCR* **2018**, *139*, 122–139; b) E. Hsu, K. Barmak, A. C. West, A.-H. A. Park, *Green Chem.* **2019**, *21*, 919–936.
[7] a) M. Kaya, *J. Waste Manag.* **2016**, *57*, 64–90; b) F. Gu, P. A. Summers, P. Hall, *J. Clean. Prod.* **2019**, *237*, 117657.
[8] a) V. Lacanau, F. Bonneté, P. Wagner, M. Schmitt, D. Meyer, F. Bihel, C. Contino-Pépin, D. Bourgeois, *ChemSusChem* **2020**, *13*, 5224–5230; b) D. Bourgeois, V. Lacanau, R. Mastretta, C. Contino-Pépin, D. Meyer, *Hydrometallurgy* **2020**, *191*, 105241.
[9] a) F. Klose, P. Scholz, G. Kreisel, B. Ondruschka, R. Kneise, U. Knopf, *Appl. Catal. B* **2000**, *28*, 209–221; b) K. A. Jantan, K. W. Chan, L. Melis, A. J. P. White, L. Marchiò, P. Deplano, A. Serpe, J. D. E. T. Wilton-Ely, *ACS Sustain. Chem. Eng.* **2019**, *7*, 12389–12398; c) G. Clavé, F. Pelissier, S. Campidelli, C. Grison, *Green Chem.* **2017**, *19*, 4093–4103.
[10] P. Ryabchuk, M. Anwar, S. Dastgir, K. Junge, M. Beller, *ACS Sustain. Chem. Eng.* **2021**, *9*, 10062–10072.
[11] P. Forster, V. Ramaswamy, P. Artaxo, T. Berntsen, R. Betts, D. Fahey, J. Haywood, J. Lean, D. Lowe, G. Raga, *CUP* **2022**.
[12] P. Gélin, M. Primet, *Appl. Catal. B* **2002**, *39*, 1–37.
[13] R. Burch, P. K. Loader, *Appl. Catal. B* **1994**, *5*, 149–164.
[14] G. Prabaharan, S. P. Barik, B. Kumar, *J. Waste Manag.* **2016**, *52*, 302–308.
[15] Y. E. Jad, G. A. Acosta, T. Govender, H. G. Kruger, A. El-Faham, B. G. de la Torre, F. Albericio, *ACS Sustain. Chem. Eng.* **2016**, *4*, 6809–6814.
[16] M. Trueba, S. P. Trasatti, *Eur JIC* **2005**, *2005*, 3393–3403.
[17] S. Touze, S. Guignot, A. Hubau, N. Devau, S. Chapron, *J. Waste Manag.* **2020**, *118*, 380–390.
[18] U. Paik, J.-G. Yeo, M.-H. Lee, V. A. Hackley, Y.-G. Jung, *Mater. Res. Bull.* **2002**, *37*, 1623–1631.
[19] M. L. Toebes, J. A. van Dillen, K. P. De Jong, *J. Mol. Catal. A Chem.* **2001**, *173*, 75–98.
[20] S. Tsubota, M. Haruta, T. Kobayashi, A. Ueda, Y. Nakahara, *Studies in Surface Science and Catalysis, Vol. 63* (Eds.: G. Poncelet, P. A. Jacobs, P. Grange, B. Delmon), Elsevier, **1991**, pp. 695–704.
[21] a) R. Gopinath, N. Lingaiah, N. Seshu Babu, I. Suryanarayana, P. S. Sai Prasad, A. Obuchi, *J. Mol. Catal. A Chem.* **2004**, *223*, 289–293; b) Y. Matsumura, M. Okumura, Y. Usami, K. Kagawa, H. Yamashita, M. Anpo, M. Haruta, *Catal. Lett.* **1997**, *44*, 189–191.
[22] a) W.-J. Shen, Y. Matsumura, *J. Mol. Catal. A Chem.* **2000**, *153*, 165–168; b) W. J. Shen, Y. Ichihashi, M. Okumura, Y. Matsumura, *Catal Letters* **2000**, *64*, 23–25; c) L.-H. Xiao, K.-p. Sun, X.-l. Xu, X.-n. Li, *Catal. Commun.* **2005**, *6*, 796–801.
[23] a) N. S. Babu, N. Lingaiah, J. V. Kumar, P. S. S. Prasad, *Appl. Catal. A* **2009**, *367*, 70–76; b) N. Seshu Babu, N. Lingaiah, P. S. Sai Prasad, *Appl. Catal. B* **2012**, *111–112*, 309–316.
[24] a) D. V. Glyzdova, T. N. Afonasenko, E. V. Khramov, N. N. Leont'eva, I. P. Prosvirin, A. V. Bukhtiyarov, D. A. Shlyapin, *Appl. Catal. A* **2020**, *600*, 117627; b) J. Liu, L. Lan, R. Li, X. Liu, C. Wu, *Int. J. Hydrog. Energy* **2016**, *41*, 951–958.
[25] a) R. N. Lamb, B. Ngamsom, D. L. Trimm, B. Gong, P. L. Silveston, P. Praserthdam, *Appl. Catal. A* **2004**, *268*, 43–50; b) A. Pachulski, R. Schödel, P. Claus, *Appl. Catal. A* **2011**, *400*, 14–24; c) Q. Zhang, J. Li, X. Liu, Q. Zhu, *Appl. Catal. A* **2000**, *197*, 221–228.
[26] a) Y. Han, G. Gu, J. Sun, W. Wang, H. Wan, Z. Xu, S. Zheng, *Appl. Surf. Sci.* **2015**, *355*, 183–190; b) F. Liao, T. W. B. Lo, S. C. E. Tsang, *ChemCatChem* **2015**, *7*, 1998–2014.
[27] a) S. Yang, A. Maroto-Valiente, M. Benito-Gonzalez, I. Rodriguez-Ramos, A. Guerrero-Ruiz, *Appl. Catal. B* **2000**, *28*, 223–233; b) D. Roth, P. Gélin, M. Primet, E. Tena, *Appl. Catal. A* **2000**, *203*, 37–45.
[28] a) H. Shinjoh, N. Isomura, H. Sobukawa, M. Sugiura in *Studies in Surface Science and Catalysis, Vol. 116* (Eds.: N. Kruse, A. Frennet, J. M. Bastin), Elsevier, **1998**, pp. 83–91; b) F. Klingstedt, H. Karhu, A. K. Neyestanaki, L. E. Lindfors, T. Salmi, J. Väyrynen, *J. Catal.* **2002**, *206*, 248–262.
[29] G. Lee, W. Zheng, K. A. Goulas, I. C. Lee, D. G. Vlachos, *Ind. Eng. Chem.* **2019**, *58*, 17718–17726.
[30] L. Mangold, H. Halleux, S. Leclerc, A. Moncomble, G. Cote, A. Chagnes, *RSC Adv.* **2021**, *11*, 27059–27073.
[31] J. Kim, G. Azimi, *RCR* **2022**, *180*, 106177.
[32] S. Brunauer, P. H. Emmett, E. Teller, *J. Am. Chem. Soc.* **1938**, *60*, 309–319.

Manuscript received: March 6, 2023
Revised manuscript received: May 31, 2023
Accepted manuscript online: May 31, 2023
Version of record online: July 20, 2023